Unusual structural tuning of magnetism in cuprate perovskites

Jorge Íñiguez[1,2] and Taner Yildirim[1]
[1] *NIST Center for Neutron Research, National Institute of Standards and Technology, Gaithersburg, MD 20899*
[2] *Dept. of Materials Science and Engineering, University of Maryland, College Park, MD 20742*

Understanding the structural underpinnings of magnetism is of great fundamental and practical interest. $Se_{1-x}Te_xCuO_3$ alloys are model systems for the study of this question, as composition-induced structural changes control their magnetic interactions. Our work reveals that this structural tuning is associated with the position of the supposedly *dummy* atoms Se and Te relative to the super-exchange (SE) Cu–O–Cu paths, and not with the SE angles as previously thought. We use density functional theory, tight-binding, and exact diagonalization methods to unveil the cause of this surprising effect and hint at new ways of engineering magnetic interactions in solids.

PACS numbers: 75.10.-b,75.30.Et,71.27.+a,75.80.+q

The $3d$ transition metal oxides are very important materials for they have been a source of novel and intriguing physical phenomena such as high-T_c superconductivity, colossal magneto-resistance, and magneto-electricity. Not surprisingly, a lot of effort is being devoted to understanding the microscopic interactions that determine the behavior of these systems. Here we are concerned with a particularly important topic, namely, the structural dependence of the magnetic couplings relevant in insulators (e.g., direct- and super-exchange). This question already received a lot of attention in early studies of magnetism in solids [1], and a renewed interest in it is being driven by current intense work on magneto-electric materials.

$Se_{1-x}Te_xCuO_3$ alloys (STCO) [2, 3] are model systems for the study of these issues. They crystallize in a perovskite structure that is strongly distorted because both Te^{+4} and Se^{+4} are relatively small. Increasing x results in structural distortions that, in turn, switch the magnetic ground state (GS) from ferromagnetic (FM) to antiferromagnetic (AFM). In Ref. [2] it is proposed that the key structural modification is related to one of the Cu–O–Cu super-exchange (SE) angles present in the system, α_2 in Fig. 1. The change in α_2 would cause the corresponding SE coupling (J_2 in Fig. 2) to switch sign, thus transforming the GS from FM to the AFM2 spin configuration of Fig. 2. This interpretation follows the spirit of the well-known Anderson-Goodenough-Kanemori (AGK) rules [1], which discuss the SE sign and strength as a function of atomic species and configurations. However, we should note that, to the best of our knowledge, there is no direct experimental evidence that AFM2 is the GS of the Te-rich alloys, as the spin structure is yet to be determined by neutron scattering measurements.

Motivated by this appealing physical picture, we decided to study the $Se_{1-x}Te_xCuO_3$ alloys using Density Functional Theory (DFT) and complementary tight-binding and many-body techniques. In this Letter we report our surprising results. We find that (i) the changes in SE angles with x have negligible influence on the corresponding couplings and (ii) what controls the magnetic interactions is the position of the presumedly *dummy* atoms Se and Te with respect to some Cu–O–Cu SE paths. Indeed, the Se/Te atoms seem to act like a *valve*, turning the AFM SE off as they approach the Cu–O–Cu group. Our results thus draw a picture of STCO that is much more subtle than that proposed in Ref. [2]. At the same time, they hint at new general ways of engineering magnetic couplings.

The calculations were performed within the generalized gradient approximation (GGA-PBE [4]) to DFT. We primarily used the all-electron implementation in the

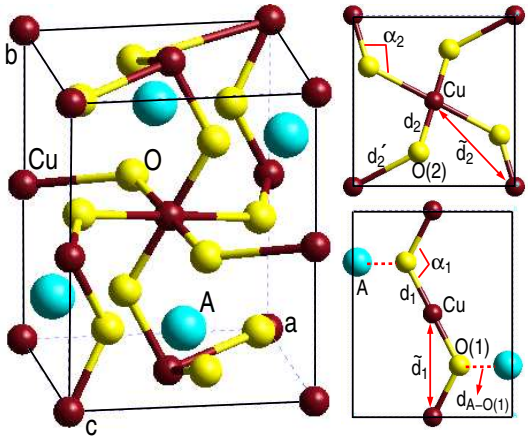

FIG. 1: Left: Unit cell of $ACuO_3$ (A=Se,Te). Right top: symmetry-equivalent Cu–O(2)–Cu groups in *ac* plane. Right bottom: Cu–O(1)–Cu chains along *b* direction. Note there are two types of oxygens in the unit cell. Relevant structural parameters are defined.

TABLE I: Structural parameters defined in Fig. 1. Values taken from Refs. [12, 13]. Distances in Angstroms and angles in degrees. Unit cell volume Ω in Å^3.

system	Ω	α_1	d_1	$\tilde{d}_1$	α_2	d_2/d_2'	$\tilde{d}_2$	$d_{A-O(1)}$
$SeCuO_3$	231	122.4	2.09	3.66	127.1	1.92/2.52	3.98	1.75
$TeCuO_3$	245	123.5	2.06	3.63	130.5	1.90/2.61	4.11	1.90

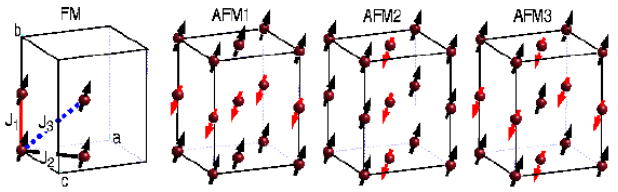

FIG. 2: Spin structures considered in this work. In the "FM" panel, only the four Cu atoms in the unit cell are shown, and the exchange constants are defined.

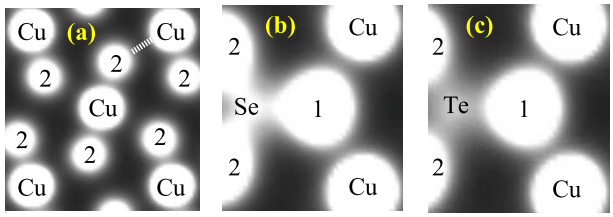

FIG. 3: Calculated spin-up charge densities. Panel a: Cu–O(2)–Cu groups in *ac* plane of $SeCuO_3$ (see Fig. 1, right top). Dashed line marks one Cu–O(2) *broken bond* (see text). Panels b and c: Cu–O(1)–Cu group and neighboring A cation, for $SeCuO_3$ and $TeCuO_3$, respectively (see Fig. 1, right bottom).

WIEN2k package [5], with a mixed basis that includes augmented plane waves and local orbitals (APW+lo). We used the LDA+U scheme to properly treat the 3*d* electrons of Cu [6, 7]. Typical cuprate values were taken for U (7.5 eV) and J (1.36 eV). We also used the ultrasoft pseudopotential [8] implementation in the PWscf package [9], with the LDA+U approach of Ref. [10] and U=6 eV. The calculation conditions [11] were converged to obtain exchange constants with an accuracy better than 1 meV. We checked that variations of 0.5-1 eV in U do not change our qualitative results. We double-checked all our results by performing both WIEN2k and PWscf calculations. In all cases we got full qualitative, and reasonable quantitative, agreement.

Raw ab initio results.– We start by considering $SeCuO_3$ (SCO) and $TeCuO_3$ (TCO) in their experimental structures [12, 13]. Both compounds have a 20-atom unit cell and differ only by small variations in atomic positions and lattice constants. The structure is shown in Fig. 1 and the relevant structural data is given in Table I.

We describe the magnetic interactions by means of a Heisenberg Hamiltonian $H = 1/2 \sum_{i,j} J_{ij} \vec{S}_i \cdot \vec{S}_j$ in which we include the exchange constants J_1, J_2, and J_3 defined in Fig. 2. (J_1 and J_2 are, respectively, associated to SE angles α_1 and α_2.) We compute the J's by requiring that this Hamiltonian reproduces, at a classical level, the energy differences between the spin configurations in Fig. 2 calculated from first-principles.

Our *ab initio* all-electron results for $SeCuO_3$ and $TeCuO_3$ are given in the first two lines of Table II. In agreement with experiment, we find FM and AFM ground states for SCO and TCO, respectively. However, the calculations predict that the GS of TCO is AFM1, and not AFM2 as proposed in Ref. [2]. Accordingly, it is J_1, not J_2, the magnetic coupling that changes sign when going from SCO to TCO. In fact, even though the change in α_1 is around three times smaller than that in α_2 (see Table I), J_1 varies by about 200% of its value, while J_2 remains almost constant. This clearly indicates that the SE angles have little influence in the magnetic couplings of these alloys. The last two lines of Table II show the results obtained when we consider $SeCuO_3$ in the $TeCuO_3$ structure (denoted by "SCO/TCO-st") and viceversa. The results confirm that it is the structure, and not chemical differences between Se and Te, what determines the magnetic GS.

TABLE II: Exchange constants of Fig. 2 calculated for various systems (see text). Values are given in meV and the magnetic ground states (GS) are indicated. The results for SCO and TCO are consistent with high-T expansion fits of the susceptibility data in Ref. [2]. In TCO there is competition between J_2 and J_3, which probably leads to interesting spin dynamics.

system	GS	J_1	J_2	J_3
SCO	FM	−4.4	−1.3	−0.8
TCO	AFM1	6.3	−1.5	−0.5
SCO/TCO-st	AFM1	17.7	−2.3	−0.6
TCO/SCO-st	FM	−14.3	1.1	−0.7

We identify the causes of these results by examining the electronic densities that come out of the calculations. Figure 3a shows the spin-up density along Cu–O(2)–Cu paths in the *ac* plane of SCO (the TCO result is essentially the same). As it is obvious, there are Cu–O(2) *broken bonds*. This is not so surprising when one notes that the *broken-bond* distance, d_2', is 2.52 Å while the other Cu–O(2) distance, d_2, is only 1.92 Å (see Table I; the values for TCO are similar). The typical Cu–O distance in cuprates is 2 Å, suggesting that in SCO and TCO the SE contribution to J_2 will be unconventional and weaker than usual. In fact, it is questionable that the above mentioned AGK rules apply in this case, and it seems reasonable that J_2 is largely independent of α_2.

Figures 3b and 3c show the spin-up charge density along the Cu–O(1)–Cu path for SCO and TCO, respectively. As far as the Cu–O distances are concerned (see Table I), this SE path is similar in both systems and a more conventional one. However, there is a structural feature that makes a big difference between SCO and TCO, namely, the position of the neighboring A cation with respect to the O(1) atom. In SCO, $d_{A-O(1)}$ is 1.75 Å, while we have 1.90 Å in TCO. Accordingly, as the density plots in Figs. 3b and 3c suggest, the Se^{+4} cation probably perturbs the O-2*p* orbitals more than Te^{+4} does. One may thus hypothesize that this pertur-

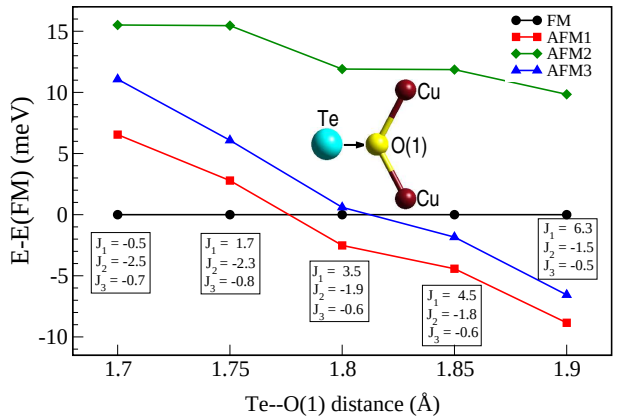

FIG. 4: Calculated energy of spin configurations defined in Fig. 2, for $TeCuO_3$, as a function of the Te–O(1) distance. FM configuration is taken as the zero of energy. Calculated exchange constants are given in meV.

bation somehow disrupts the SE mechanism and renders a FM J_1 in SCO, while regular SE results in an AFM J_1 in TCO. To check this conjecture, we calculated the magnetic interactions in TCO as a function of the Te–O(1) distance. The results in Fig. 4 show that, indeed, when Te comes close enough to O(1) (about 1.75 Å), a FM GS results and J_1 switches sign. This is very strong evidence that we have identified the structural feature that controls the magnetic ground state in $Se_{1-x}Te_xCuO_3$ alloys.

Tight-binding analysis.– Great insight can be gained into the ultimate causes of these effects by discussing them in terms of the relevant electronic interactions in the system (i.e., hoppings, Coulomb, and exchange). To do so, we have implemented a simple and powerful scheme to compute tight-binding (TB) Hamiltonians that reproduce the first-principles electronic structure. In the following we sketch the method.

Consider the atomic orbitals (AO's) of an isolated atom κ. Let us bring those AO's into the crystal and call them $\phi^{\mathbf{R}}_{\kappa\alpha}$, where $\mathbf{R}$ is a lattice vector and α stands for the quantum numbers $\{n,l,m\}$. The corresponding Bloch-like wave function is $\phi^{\mathbf{k}}_{\kappa\alpha} = \sum_{\mathbf{R}} e^{i\mathbf{k}\mathbf{R}}\phi^{\mathbf{R}}_{\kappa\alpha}$, where $\mathbf{k}$ is in the Brillouin zone (BZ). Let $\psi_{\mathbf{k}j}$ and $E_{\mathbf{k}j}$ denote, respectively, the eigenstates and eigenvalues of the Kohn-Sham Hamiltonian ($\hat{H}^{\rm KS}$) at $\mathbf{k}$. We define

$$|\widetilde{\phi}^{\mathbf{k}}_{\kappa\alpha}\rangle \;\equiv\; f\sum_j |\psi_{\mathbf{k}j}\rangle\langle\psi_{\mathbf{k}j}|\phi^{\mathbf{k}}_{\kappa\alpha}\rangle\;, \qquad (1)$$

where f is a normalization factor and the band index j runs over a set of bands that we are free to choose. We now perform the well-known Löwdin-Mattheiss transformation to obtain orthonormal wave functions

$$|\widehat{\phi}^{\mathbf{k}}_{\kappa\alpha}\rangle \;=\; \sum_j |\psi_{\mathbf{k}j}\rangle\Big[\sum_{\kappa'\alpha'}(S^{\mathbf{k}})^{-1/2}_{\kappa'\alpha';\kappa\alpha}\langle\psi_{\mathbf{k}j}|\phi^{\mathbf{k}}_{\kappa'\alpha'}\rangle\Big]\;, \qquad (2)$$

where $(S^{\mathbf{k}})^{-1/2}$ is derived from the overlap matrix of the $\widetilde{\phi}^{\mathbf{k}}$'s as described in Ref. [14]. Then, we can easily compute the associated Wannier functions (WF's) $\widehat{\phi}^{\mathbf{R}}_{\kappa\alpha}$ and the parameters of the corresponding TB Hamiltonian:

$$\langle\widehat{\phi}^{\mathbf{R}}_{\kappa\alpha}|\hat{H}^{\rm KS}|\widehat{\phi}^{\mathbf{R}'}_{\kappa'\alpha'}\rangle = \frac{1}{N}\sum_{\mathbf{k}} e^{i\mathbf{k}(\mathbf{R}-\mathbf{R}')}\sum_j E_{\mathbf{k}j}(C^{\mathbf{k}}_{j;\kappa\alpha})^* C^{\mathbf{k}}_{j;\kappa',\alpha'}\;, \qquad (3)$$

where the C's are the bracketed coefficients in Eq. (2) and N is the number of k-points in the BZ.

If in the above sums we include a *small* number of bands (e.g., the nominal Cu-3d and O-2p bands), the resulting WF's will significantly differ from original AO's ϕ and incorporate the effects of the surrounding lattice. The more additional bands we include, the more the WF's will resemble the isolated-atom orbitals. Note also that, by construction, our TB Hamiltonians can reproduce the electronic band structure with arbitrary precision, the only limitation being the spatial cutoff beyond which the hoppings are neglected in practice [15].

We used this scheme to construct TB Hamiltonians for the non-spin-polarized band structures of SCO and TCO obtained from pseudopotential calculations. We considered all valence and low-lying conduction bands, as we were interested not only in the Cu-3d–O-2p couplings, but also in how those are modified by the A cations. The resulting WF's are very close to the isolated-atom AO's.

The Cu-3d–O-2p hoppings along the J_2 SE path are very asymmetric, as the two Cu–O(2) distances differ greatly. For the *broken-bond* pair, we obtain a maximum hopping of 0.35 eV, while we get 0.85 eV for the other Cu–O(2) pair. (These are results for SCO. The situation is similar in TCO.) This quantitatively confirms that the SE contribution to J_2 will be relatively small.

Regarding the other SE path, the two Cu–O(1) pairs are equivalent by symmetry, and the maximum Cu-3d–O-2p hopping is 0.77 eV in SCO and 0.87 eV in TCO. On the other hand, the maximum Se-4s–O(1)-2p hopping is 4.51 eV in SCO, while for Te-5s–O(1)-2p in TCO we get 3.65 eV. These results indicate a relatively strong Se-4s–O-2p interaction in SCO, which results in 3d–2p hoppings about 10% smaller than the corresponding ones in TCO. One can thus infer that the SE contribution to J_1 will be smaller in SCO than in TCO.

Many-body analysis.– Our first-principles TB Hamiltonians can be supplemented with Coulomb and exchange terms to obtain realistic models of the electronic interactions. The resulting Hubbard-like Hamiltonians make it possible to isolate the various contributions to the magnetic couplings (direct-exchange, SE), and thus identify the mechanisms behind them. Here we focus on the description of the low-energy spin excitations in particular Cu–O–Cu groups, where the magnetic interaction is described by a single exchange constant J (this will be J_1 or J_2 if we consider, respectively, Cu–O(1)–Cu or Cu–O(2)–Cu). The many-body states are constructed by distributing two holes among the Cu-3d and O-2p orbitals. We di-

agonalize the resulting Hamiltonian matrix and compute J from the energy gap between the lowest-lying singlet and triplet states.

We added the following terms to our first-principles TB Hamiltonians: on-site Coulomb interactions for both Cu-3d and O-2p electrons, on-site exchange for the O-2p electrons (which implements Hund's first rule), and inter-site exchange between Cu-3d electrons (which is well-known to favor FM interactions). The resulting Hamiltonians are a simplification of that in Eq. (4) of Ref. [16]. We retained the above terms partly guided by numerical evidence that they have the biggest effect in the J's. We treated all Cu-3d and all O-2p orbitals equally, so that the model has only four parameters, namely, Coulomb U_d and U_p, and exchange K_p and K_{dd}.

By choosing reasonable values of these parameters, we were able to obtain J_1 and J_2 exchange constants in qualitative agreement with the first-principles results for both SCO and TCO. We employed parameters in the following ranges: U_d=8-9 eV, U_p=5-6 eV, K_p=1-2 eV, and K_{dd}=8.5-12.5 meV. We imposed the constraint that K_{dd} is consistent with the Cu–Cu distance, i.e., we used larger values for smaller distances. Our analysis led us to two main conclusions. (i) In all the cases, the SE couplings *per se* result in AFM interactions. The inter-site exchange K_{dd} is necessary to obtain FM J's. (ii) The structural changes tune the magnetic couplings via their effect on the magnitude of the Cu-3d–O-2p hoppings. Smaller hoppings result in a smaller SE singlet-triplet splitting and, thus, make it easier for the K_{dd} interaction to turn the coupling FM. Given the drastic approximations underlying our Hubbard-like Hamiltonians, and the fact that the U and K parameters were not calculated *ab initio*, these conclusions should be taken with caution. Nevertheless, they are consistent with our body of results and make physical sense.

In summary, we have studied the $Se_{1-x}Te_xCuO_3$ alloys in which the magnetic interactions are controlled by composition-dependent structural changes. We employed three complementary approaches, i.e., LDA+U, tight-binding, and exact diagonalization of effective Hamiltonians for finite clusters, which allowed us to study the magnetic interactions in great detail. We find that the key structural feature is the position of the supposedly *dummy* atoms Se and Te relative to Cu–O–Cu SE paths. As the Se/Te atom approaches the Cu–O–Cu group, it acts like a magnetic *valve* and reduces the SE contribution to the magnetic coupling. We find SE favors antiferromagnetism and, thus, this decrease allows direct exchange between Cu-3d electrons to render a ferromagnetic interaction. This is quite a surprising mechanism, as a more conventional one related to the SE angles might have been expected and, in fact, was proposed in the literature [2]. On the other hand, this effect could well lead to novel ways of engineering magnetic couplings in solids. Our work shows that complex magnetic interactions may underlay seemingly simple phenomena, and highlights the usefulness of *ab initio* studies.

It would be interesting to confirm experimentally the magnetic ground state of $TeCuO_3$ that we predict. Also, we expect that application of external pressure on $TeCuO_3$ could allow to tune the magnetic couplings in the way shown here. Finally, we are currently investigating other perovskites (e.g., $MTiO_3$, with M=Y, La) to check whether similar effects occur.

We thank Art Ramirez, Collin Broholm, and David Vanderbilt for useful comments.

[1] P.W. Anderson, Solid State Phys. **14**, 99 (1963).
[2] M.A. Subramanian, A.P. Ramirez, and W.J. Marshall, Phys. Rev. Lett. **82**, 1558 (1999).
[3] G. Lawes, A.P. Ramirez, C.M. Varma, and M.A. Subramanian, Phys. Rev. Lett. **91**, 257208 (2003).
[4] J.P. Perdew, K. Burke, and M. Ernzerhof, Phys. Rev. B **77**, 3865 (1996).
[5] See K. Schwarz, P. Blaha, and G.K.H. Madsen, Comp. Phys. Comm. **147**, 71 (2002), and references therein.
[6] V.I. Anisimov, J. Zaanen, O.K. Andersen, Phys. Rev. B **44**, 943 (1993).
[7] A.I. Liechtenstein, V.I. Anisimov, J. Zaanen, Phys. Rev. B **52**, 5467 (1995).
[8] D. Vanderbilt, Phys. Rev. B **41**, 7892 (1990).
[9] S. Baroni, A. Dal Corso, S. de Gironcoli, and P. Giannozzi, http://www.pwscf.org.
[10] M. Cococcioni and S. de Gironcoli, cond-mat/0405160.
[11] More technical details follow. Brillouin zone integrals: tetrahedron method, 4×4×3 grid. WIEN2k details follow. Semicore orbitals: Cu 3s and 3p, Se 3d, and Te 4p and 4d. Muffin-tin sphere radii: $R_{\rm Cu}$=$R_{\rm Se}$=1.8 a.u. and $R_{\rm O}$=1.4 a.u. for $SeCuO_3$; $R_{\rm Cu}$=$R_{\rm Te}$=1.9 a.u. and $R_{\rm O}$=1.6 a.u. for $TeCuO_3$. For modified structures, smaller values used as needed. Plane-wave cutoff $K_{\rm max} = 7/R_{\rm min}$. PWscf details follow. Valence orbitals: Te 4d, 5s and 5s, Se 3d, 4s and 4p, Cu 3d and 4s, and O 2s and 2p. Partial core corrections used. Plane-wave cutoff: 30 Ry.
[12] K. Kohn, K. Inoue, O. Horie, and S. Akimoto, J. Sol. St. Chem. **18**, 27 (1976).
[13] E. Philippot and M. Maurin, Rev. Chim. Minerale **13**, 162 (1976).
[14] L.F. Mattheiss, Phys. Rev. B **2**, 3918 (1970).
[15] Marzari and Vanderbilt [Phys. Rev. B **56**, 12847 (1997)] used a similar scheme, with gaussians instead of AO's, to obtain initial guesses of their "maximally localized" WF's. Recently, Ku, Rosner, Pickett, and Scalettar [Phys. Rev. Lett. **89**, 167204 (2002)] employed such WF's to derive first-principles many-body Hamiltonians. Let us add that we obtain fairly localized WF's when a small number of bands (e.g., the nominal Cu-3d and O-2p bands) are used in the calculation (Eq. (1)). Moreover, this construction method allows to extract the bands of interest in entangled-band situations and control the transformation properties of the resulting WF's.
[16] T. Yildirim, A.B. Harris, A. Aharony, and O. Entin-Wohlman, Phys. Rev. B **52**, 10239 (1995).